Accurate numerical method for the calculation of doubly excited states in atoms

M. A. Albert, S. Laulan and S. Barmaki

Laboratoire de Physique Computationnelle et Photonique, Université de Moncton Campus de Shippagan, 218 boulevard J. D. Gauthier, E8S 1P6 Shippagan, New-Brunswick, Canada

Abstract.

We report in this paper computed values of the energy positions and widths of the lowest $^1P^o$ singlet doubly excited states of the helium atom. The results are obtained by a direct numerical solution of the time-independent Schrödinger equation using a discretization technique with B-spline functions combined with complex rotation method. The present approach has the numerical advantage to generate accurate energy positions and widths in a single calculation. The computed data are in very good agreement with results from other theoretical approaches.

Nous reportons dans cet article nos résultats concernant les positions et largeurs énergétiques des états singulets doublement excités de symétrie $^1P^o$ de l'atome d'hélium. Nos résultats sont obtenus par la résolution numérique directe de l'équation de Schrödinger indépendante du temps avec une technique de discrétisation basée sur les fonctions B-splines combinée avec une méthode de rotation complexe. Notre méthode numérique a pour avantage de générer de façon très précise les positions et largeurs énergétiques en un seul calcul. Nos résultats sont en très bon accord avec les résultats issus d'autres approches théoriques.

1. INTRODUCTION

The electron-electron interaction in the helium atom produces a large number of doubly excited states embedded between the $He^+(N\ell)$ hydrogenic thresholds. These states, discovered by Madden and Codling [1, 2] in their pioneering experimental work on the photoabsorption of the helium atom, can decay by electron emission (autoionization). An autoionizing state is characterized by its position energy E and by its width Γ which is related to its lifetime τ as $\Gamma = \hbar/\tau$.

The recent advent of free electron lasers (FELs) sources such as the Free Electron laser Radiation for Multidisciplinary Investigations (FERMI) [3] in Trieste, Italy, or the Free electron LASer at Hambourg (FLASH) [4], Germany, opens a new opportunity to investigate laser-atom processes involving autoionizing states by single coherent pulses. Such pulses offer the possibility to directly address autoionizing $^1P^o$ states from the ground state of the atom by one-photon absorption. Besides, the durations of the exciting pulses can be made comparable to the atomic autoionizing states lifetimes, which will allow to observe and manipulate Fano interferences. An adequate analysis of the autoionization dynamics requires an accurate description of the energy positions and lifetimes of autoionizing $^1P^o$ states in the investigated target atom.

We present in this paper an accurate description of the singlet doubly excited states of the helium atom. Our theoretical approach is based on the numerical solution of the time-independent Schrödinger equation with a complex rotation me-thod [5–7]. The radial two-electron wave function is expanded on antisymmetrized products of B-spline functions [8]. The electron-electron correlation is described with a high degree of accuracy as the electrostatic interaction potential $1/r_{12}$ is treated without any approximation by using the multipole expansion of the Coulomb repulsion between the two electrons. The present method enables to compute the resonances energies and the corresponding lifetimes precisely and simultaneously.

Atomic units (a.u.), i.e., $e = m = \hbar = 1$ and $c = \frac{1}{\alpha}$, are used throughout this paper unless otherwise stated.

2. THEORETICAL APPROACH

The nonrelativistic Hamiltonian for the two electrons of the helium atom is given by :

$$H = \sum_{i=1}^{2} \Big(-\frac{1}{2}\Delta_i - \frac{2}{r_i} \Big) + \frac{1}{r_{12}}, \tag{1}$$

where $r_{12} = |\mathbf{r_1} - \mathbf{r_2}|$ denotes the interelectronic distance. The electrostatic interaction potential $1/r_{12}$ is treated by using the multipole expansion of the Coulomb repulsion between the two electrons [9]:

$$\frac{1}{r_{12}} = \sum_{\ell=0}^{\infty} \frac{4\pi}{(2\ell+1)} \sum_{m=-\ell}^{\ell} \frac{r_<^\ell}{r_>^{\ell+1}} Y_\ell^{m^*}(\Omega_1) Y_\ell^m(\Omega_2), \tag{2}$$

with $r_< = min(r_1, r_2)$, $r_> = max(r_1, r_2)$ and $Y_\ell^m(\Omega_i)$ denotes a spherical harmonic with $\Omega_i = (\theta_i, \varphi_i)$. The time-indep-endent Schrödinger equation (TISE) describing the motion of the valence electrons is given by:

$$H\Phi^{SLM}(\mathbf{r}_1, \mathbf{r}_2) = E\Phi^{SLM}(\mathbf{r}_1, \mathbf{r}_2). \tag{3}$$

The spatial wave function $\Phi^{SLM}(\mathbf{r}_1, \mathbf{r}_2)$ is expanded on the basis of two-electron configurations that are products of one-electron functions, as follows :

$$\begin{aligned}\Phi^{SLM}(\mathbf{r}_1, \mathbf{r}_2) = \\ \sum_{\alpha \equiv \ell_1, \ell_2, i, j} c_{i,j}^{\ell_1, \ell_2, SLM} \left[\frac{B_i^k(r_1)}{r_1} \frac{B_j^k(r_2)}{r_2} \mathcal{Y}_{\ell_1,\ell_2}^{L,M}(\Omega_1, \Omega_2) \right. \\ \left. + (-1)^S \frac{B_i^k(r_2)}{r_2} \frac{B_j^k(r_1)}{r_1} \mathcal{Y}_{\ell_1,\ell_2}^{L,M}(\Omega_2, \Omega_1) \right]\end{aligned} \tag{4}$$

for a total spin S ($S = 0$, 1), a total angular momentum L and projection M. $l_1(l_2)$ is the orbital angular momentum quantum number of electron 1 (2). The radial function $B_i^k(r)\ |_{i=1,\cdots,N_b}$ is a B-spline of order k, i.e. a piecewise polynomial of degree $k-1$ [8]. N_b is the number of B-splines used per electron. Although the Hamiltonian in Eq. (1) is spin-independent, the spin effects are taken into account in Eq. (4). The Pauli exclusion principle states that the total wave function that is the product of the spatial wave function $\Phi^{SLM}(\mathbf{r}_1, \mathbf{r}_2)$ and the spin wave function $\chi^{S;M_S=-S,0,S}(1,2)$ must be antisymmetric. For $S = 0$, the spin wave function is antisymmetric (singlet), while for $S = 1$ the three spin functions are symmetric (triplet). The expression of $\Phi^{SLM}(\mathbf{r}_1, \mathbf{r}_2)$ ensures that the spatial function will be symmetric for $S = 0$ or antisymmetric for $S = 1$. The angular part of the wave function defined in Eq. (4) is described by the bipolar spherical harmonic function $\mathcal{Y}_{\ell_1,\ell_2}^{L,M}(\Omega_1, \Omega_2)$ [9]:

$$\begin{aligned}\mathcal{Y}_{\ell_1,\ell_2}^{L,M}(\Omega_1, \Omega_2) = \sum_{m_1=-\ell_1}^{\ell_1} \sum_{m_2=-\ell_2}^{\ell_2} (-1)^{\ell_1-\ell_2+M} \sqrt{2L+1} \\ \times \begin{pmatrix} \ell_1 & \ell_2 & L \\ m_1 & m_2 & -M \end{pmatrix} Y_{\ell_1}^{m_1}(\Omega_1) Y_{\ell_2}^{m_2}(\Omega_2).\end{aligned} \tag{5}$$

The angular configurations (ℓ_1, ℓ_2) employed in Eq. (5) are determined by the triangle condition $|\ell_1 - \ell_2| \leq L \leq |\ell_1 + \ell_2|$.

We use the complex rotation method [5–7] to compute the resonances in helium atom. The method has the advantage to generate the parameters of the autoionizing resonances embedded between the hydrogenic thresholds in a single calculation. The technique consists in applying a rotation by an angle θ to the radial coordinates $r_i \rightarrow r_i\ e^{i\theta}$ in the complex plane, which transforms H into the following non-Hermitian operator given by

$$H(\theta) = \sum_{i=1}^{2} \Big(-\frac{1}{2}\Delta_i e^{-2i\theta} - \frac{2}{r_i} e^{-i\theta} \Big) + \frac{1}{r_{12}} e^{-i\theta}. \tag{6}$$

The TISE equation then transforms to

$$H(\theta)\Phi_\theta^{SLM}(\mathbf{r}_1, \mathbf{r}_2) = E_\theta \Phi_\theta^{SLM}(\mathbf{r}_1, \mathbf{r}_2). \tag{7}$$

The diagonalization of Eq. (7) generates the whole electronic structure of the helium atom. The obtained eigenvalues E_θ and eigenvectors Φ_θ are complex.

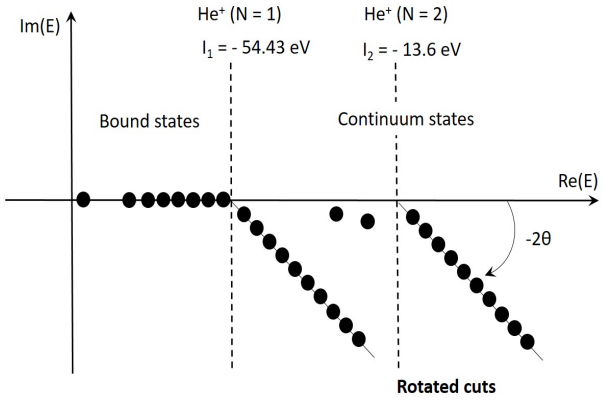

Figure 1. Schematic description of the complex energy spectrum generated by the complex rotation method.

A schematic description of the complex energy spectrum of He generated by the complex rotation method is depicted in Fig. 1. The spectrum separates into three categories easily distinguishable :

(i) Bound states : their energies are identical to the unrotated Hamiltonian H of Eq. (1) for $\theta \leq \pi/2$.

(ii) Nonresonant continuum states : their energies are rotated downwards by an angle -2θ around the $\mathrm{He}^+(N\ell)$ hydrogenic thresholds $\mathrm{I}_N = -\frac{54.43}{N^2}$ eV.

(iii) Resonant states : they are embedded in the single continua above the first $\mathrm{He}^+(1s)$ hydrogenic threshold $\mathrm{I}_1 = -\,54.43$ eV. The discrete complex eigenvalue of a resonant state has the form $E_{res} = E - i\frac{\Gamma}{2}$, where E and Γ are the resonance position and width, respectively. These resonances become exposed (uncovered by the cuts) once the rotation angle θ is greater than $\frac{1}{2} arg(E_{res})$.

3. Results and discussion

Doubly excited states form many different series that are embedded between the $\mathrm{He}^+(N\ell)$ hydrogenic thresholds. These resonant states can decay by autoionization due to the strong electrostatic interaction between the two electrons. In this section,

States $^1L^\pi$	Our results (eV)	NIST values (eV)
$^1S^e(1)$	-78.99641	-79.00515
$^1P^o(1)$	-57.79181	-57.78712
$^1P^o(2)$	-55.92335	-55.91813
$^1P^o(3)$	-55.26842	-55.26308
$^1P^o(4)$	-54.96342	-54.95935
$^1P^o(5)$	-54.76196	-54.79414

Table 1. Our computed energies of the $^1S^e$ ground state and the lower $^1P^o$ singly excited states lying below the first $He^+(1s)$ hydrogenic threshold $I_1 = -54.43$ eV. The results are compared with the experimental measurements from NIST [12].

we report accurate data of the resonant parameters of singlet $^1P^\pi$ doubly excited states of odd-parity ($\pi = o$) located below the $N = 2$ threshold. The data are generated for total orbital angular momentum $L = 1$ by the numerical resolution of Eq. (7). We considered in our calculations the atomic system confined in a spherical box of radius $r_0 = 90$ a.u. In the radial part of the expansion (4), $N_b = 110$ B-spline functions of order $k = 7$ are used per electron. We took into account, in the angular part of the expansion, the pairs $(\ell_1 = 0, \ell_2 = 1)$, $(\ell_1 = 1, \ell_2 = 2)$ and $(\ell_1 = 2, \ell_2 = 3)$ that satisfy the parity $\pi = (-1)^{\ell_1+\ell_2} = (-1)^L$. We have considered in total 36 300 (ℓ_1, ℓ_2, i, j) combination terms in the expansion (4) to ensure an accurate representation of the bound and continuum energy spectrum of the atom. An accurate treatment of the electron-electron correlation is necessary to correctly describe the strong electrostatic interaction between the electrons in doubly excited states. The discretization technique with B-spline functions we used allows a rapid and accurate calculation of the electrostatic interaction term $1/r_{12}$ (Eq. (2)). An accurate description of the continuum states is also necessary in order to adequately describe the strength of the coupling of the resonant states to the adjacent continuum states. The flexibility of the B-spline functions allows to control the density of the continuum states which ensures the accuracy of the calculation of the resonant parameters. More details about the efficiency of B-spline functions in the calculations of atomic and molecular field-free energy spectra are given in our previous works [10, 11] and references therein. We have checked the numerical stability of the computed data by varying the number of B-spline functions and the radial box size. The convergence of the results is obtained for values of θ in the interval $[0.09, 0.25]$ rad.

In Table 1, we present our computed energy positions of the $^1S^e$ ground state and the lower $^1P^o$ singly excited states in He obtained by the diagonalization of Eq. (7) with $\theta = 0.2$ rad. These results are in very good agreement with the experimental measurements from the National Institute of Standards Technology database (NIST) [12]. The diagonalization provides the whole spectrum of bound and continuum electronic states where the doubly excited states are easily detectable with simultaneous calculations of their energy positions E and the corresponding widths Γ. Various

$^{2S+1}L^{\pi}$	$^1P^o$ (1)	$^1P^o$ (2)	$^1P^o$ (3)	$^1P^o$ (4)
		$-E$ (eV)		
Present	18.852	16.247	15.348	14.885
Eiglsperger et al. [16]	18.861	16.247	15.349	14.887
Ho [17]	18.861	16.247	15.349	14.887
Oza [19]	18.852	16.247	15.348	—
Bhatia and Temkin [20]	18.855	16.247	15.344	—
Macias and Riera [18]	18.834	16.253	15.342	14.885
		Γ (eV)		
Present	3.73[-02]	1.04[-04]	8.16[-03]	1.58[-06]
Eiglsperger et al. [16]	3.75[-02]	1.04[-04]	8.16[-03]	<0.5[-06]
Ho [17]	3.73[-02]	1.05[-04]	8.19[-03]	0.43[-06]
Oza [19]	3.62[-02]	1.06[-04]	8.43[-03]	—
Bhatia and Temkin [20]	3.63[-02]	1.06[-04]	9.00[-03]	—
Macias and Riera [18]	3.74[-02]	1.43[-04]	8.45[-03]	3.03[-05]

$^{2S+1}L^{\pi}$	$^1P^o$ (5)	$^1P^o$ (6)	$^1P^o$ (7)	$^1P^o$ (8)
		$-E$ (eV)		
Present	14.870	14.540	14.356	14.348
Eiglsperger et al. [16]	14.871	14.541	14.357	14.348
Ho [17]	14.871	14.541	14.357	14.348
Oza [19]	14.870	14.540	—	14.348
Bhatia and Temkin [20]	—	—	—	—-
Macias and Riera [18]	14.861	14.538	14.355	14.343
		Γ (eV)		
Present	5.17[-05]	3.48[-03]	2.12[-07]	2.50[-05]
Eiglsperger et al. [16]	5.22[-05]	3.48[-03]	< 3.81[-06]	2.50[-05]
Ho [17]	5.58[-05]	3.51[-03]	—	—
Oza [19]	5.65[-05]	3.37[-03]	—	2.77[-05]
Bhatia and Temkin [20]	—	—	—	—
Macias and Riera [18]	2.10[-05]	3.62[-03]	1.28[-05]	1.03[-05]

Table 2. Energy positions E and widths Γ for $^1P^o$ doubly excited states of He. Numbers in square brackets represent powers of ten.

classifications schemes have been introduced to categorize these states in two-electron systems [13–15]. In this paper, we simply identified the doubly excited states by their total symmetry, energy and width.

Our computed data of the energy positions and widths for the eight lowest singlet doubly excited $^1P^o$ resonances located below the $N = 2$ threshold are displayed in Table 2. We compare the obtained results with existing data from calculations based on other different theoretical approaches. The reported data of Eiglsperger et al. [16] and Ho [17] were also generated with complex rotation method (CRM) but with the use of different type of mathematical functions to construct the two-electron wave functions. Eiglsperger et al. [16] have expanded the two-electron wave functions in a complete basis of Sturmian type functions, while Ho [17] used Hylleraas-type wave functions to determine the resonant parameters of the four lower states and Slater-type-orbital (STO) basis sets for the high-lying resonances. We also compare in Table 2 our results with data obtained from other theoretical approaches not based on CRM where the energy positions and widths are generated in two separate steps. The results of Macias and Riera [18] are from calculations based on the Feshbach formalism with a discrete method using STO basis sets, while those of Oza [19] are from close-coupling calculations also employing STO basis sets to expand the two-electron wave functions. Table 2 also shows reported data from Bhatia and Temkin [20]. The authors have obtained the energy positions with a variational procedure along with Feshbach-projection formalism and Hylleraas-type wave functions. They have used the static-exchange approximation to calculate the continuum waves to obtain the widths. By comparing our data of the resonant parameters displayed in Table 2 with the other data, we notice the very good agreement we have with the energy positions of Eiglsperger et al. [16], Ho [17] and Oza [19]. The results of the positions are also in a good agreement with Macias and Riera [18] and the available data of Bhatia and Temkin [20]. The doubly excited $^1P^o$ states differ by their associated widths; the $^1P^o(1)$, $^1P^o(3)$ and $^1P^o(6)$ states have broad widths, the $^1P^o(2)$, $^1P^o(5)$ and $^1P^o(8)$ have narrow widths and the $^1P^o(4)$ and $^1P^o(7)$ have very narrow widths. The computed widths of the broad resonances $^1P^o(1)$, $^1P^o(3)$ and $^1P^o(6)$ compare very well with the results of Eiglsperger et al. [16] and Ho [17]. They also are in a good agreement with the reported data of Oza [19], Macias and Riera [18] and the available data of Bhatia and Temkin [20]. In contrast with the agreement about the widths of broad resonances, slight or large differences can be observed in Table 2 between the values of the width of the narrow and very narrow resonances. Our numerical method succeeds in generating the narrow widths of the $^1P^o(2)$, $^1P^o(5)$ and $^1P^o(8)$ that are in excellent agreement with Eiglsperger et al. [16] and in good agreement with the data of Ho [17] and Oza [19]. The width of the $^1P^o(2)$ state calculated by Macias and Riera [18] is slightly larger than our result, whereas the widths they obtained for the $^1P^o(5)$ and $^1P^o(8)$ are lower. The present method also describes accurately the very narrow widths of the $^1P^o(4)$ and $^1P^o(7)$ states. We notice that the widths reported by Macias and Riera [18] for these states are larger than ours and those of Eiglsperger et al. [16].

The numerical approach developed in this paper generates data of the energy positions that are in a good agreement with the available data from the other theoretical approaches. Some of these approaches, although efficient in describing lowest doubly excited states, have shown some limitations in calculating the resonant parameters of high lying $^1P^o$ resonances, especially those with narrow and very narrow widths. The width values obtained by our numerical approach agree best with the reported data from calculations based on Sturmian type functions [16] and Hylleraas-type wave functions [17].

4. Conclusion

We have computed the resonant parameters of singlet $^1P^o$ doubly excited states of the helium atom by numerically solving the time-independent Schrödinger equation with a complex rotation method. The discretization technique with B-spline functions used in this paper allows an accurate description of the electron-electron interaction and the continuum which ensures a precise calculations of the resonant parameters. The use of B-spline functions combined with complex rotation method has the numerical advantage to generate accurate energy positions and widths in a single calculation. The computed data are in very good agreement with results from other theoretical approaches. The numerical approach presented in this paper could be adapted for time-dependent calculations to investigate the dynamic of the autoionization process triggered by one-photon absorption from the ground state of the helium atom. The exciting laser pulse will be in this case of duration comparable to the computed lifetimes of the lowest autoionizing states. An investigation that could help to improve our understanding of how to control Fano interferences by intense and short laser pulses.

Acknowledgements

The present research was supported by the Natural Sciences and Engineering Research Council (NSERC) and by the New Brunswick Innovation Foundation (NBIF). Allocation of CPU time and assistance with the computer facilities from Compute Canada are acknowledged.

References

[1] R. Madden, and K. Codling, Phys. Rev. Lett. **10**, 516 (1963).
[2] R. Madden, and K. Codling, Astrophys. J. **1141**, 364 (1965).
[3] Home page of FERMI at Elettra in Trieste, Italy, https://www.elettra.trieste.it/lightsources/fermi/machine.htlm.
[4] Home page of FLASH in Hambourg, Germany, http://flash.desy.de.
[5] J. Aguilar, and J. Combes, Commun. Math. Phys. **22**, 269 (1971).
[6] E. Balslev, and J. Combes, Commun. Math. Phys. **22**, 2280 (1971).
[7] B. Simon, Commun. Math. Phys. **27**, 1 (1972).
[8] C. de Boor, *A Practical Guide to Splines* (Springer, New York, 1978).

[9] R. N. Zare, *Angular Momentum: Understanding spatial Aspects in Chemistry and Physics* (Wiley Interscience, 1988).
[10] S. Barmaki, H. Bachau, and M. Ghalim, Phys. Rev. A **69**, 043403 (2004).
[11] S. Barmaki, P. Lanteigne, and S. Laulan, Phys. Rev. A **89**, 063406 (2014).
[12] A. Kramida, Yu Ralchenko, J. Reader and NIST ASD team 2017, *NIST Atomic Spectra Database* (ver. 5.5.1), available at: http://physics.nist.gov/asd (December 21, 2017), National Institute of Standards and Technology, Gaithersburg, MD.
[13] M. Conneely, and L. Lipsky, J. Phys. B: At. Mol. Opt. Phys.Phys. **1**, 4135 (1978).
[14] D. R. Herrick, and O. Sinanoglu, Phys. Rev. A **11**, 97 (1975).
[15] C. D. Lin, Phys. Rev. Lett. **51**, 1348 (1983).
[16] J. Eiglsperger, M. Schronwetter, B. Piraux, and J. Madronero, At. Data Nucl. Data Tables **98**, 120 (2012).
[17] Y. Ho, Z. Phys. D: At. Mol. Clusters **21**, 192 (1991).
[18] A. Macias, and A. Riera, Phys. Lett. A **119**, 28 (1986).
[19] D. Oza, Phys. Rev. A **33**, 824 (1986).
[20] A. Bhatia and A. Temkin, Phys. Rev. A **29**, 1895 (1984).